



OPEN Towards optimised extracellular vesicle proteomics from cerebrospinal fluid

Petra Kangas^{1✉}, Tuula A. Nyman², Liisa Metsähonkala³, Cameron Burns⁴, Robert Tempest⁴, Tim Williams⁵, Jenni Karttunen^{1,7} & Tarja S. Jokinen^{1,6,7}

The proteomic profile of extracellular vesicles (EVs) from cerebrospinal fluid (CSF) can reveal novel biomarkers for diseases of the brain. Here, we validate an ultrafiltration combined with size-exclusion chromatography (UF-SEC) method for isolation of EVs from canine CSF and probe the effect of starting volume on the EV proteomics profile. First, we performed a literature review of CSF EV articles to define the current state of art, discovering a need for basic characterisation of CSF EVs. Secondly, we isolated EVs from CSF by UF-SEC and characterised the SEC fractions by protein amount, particle count, transmission electron microscopy, and immunoblotting. Data are presented as mean \pm standard deviation. Using proteomics, SEC fractions 3–5 were compared and enrichment of EV markers in fraction 3 was detected, whereas fractions 4–5 contained more apolipoproteins. Lastly, we compared starting volumes of pooled CSF (6 ml, 3 ml, 1 ml, and 0.5 ml) to evaluate the effect on the proteomic profile. Even with a 0.5 ml starting volume, 743 ± 77 or 345 ± 88 proteins were identified depending on whether 'matches between runs' was active in MaxQuant. The results confirm that UF-SEC effectively isolates CSF EVs and that EV proteomic analysis can be performed from 0.5 ml of canine CSF.

Extracellular vesicle (EV) is an umbrella term for various kinds of cell-released membranous particles. Traditional EV subtypes include exosomes, that are secreted from endosomal pathway, microvesicles from plasma membrane budding, and apoptotic bodies released mainly during cell death^{1,2}. Recently, other extracellular nanoparticles, including small (< 50 nm) non-membranous exomeres and supermeres have also been discovered^{3–5}. Alternative EV subgroups have been classified based on the size and density of the particles since these are properties that can be used to fractionate EVs^{1,6}.

EVs are a promising tool for biomarker discovery, since EV cargo reflects that of the cells the EVs are secreted from, and it is possible to isolate them from different biofluids. Cerebrospinal fluid (CSF) is a liquid located close to the central nervous system and is secreted mostly by cells in the choroid plexus^{7–9}. An important role of EVs has been demonstrated for the central nervous system, such as regulation of synaptic communication, synaptic strength, and nerve regeneration^{10,11}. Thus, analysis of EVs secreted into CSF can offer a way to study changes in brain tissue. So far changes in CSF EV cargo have been detected in patients with Alzheimer's disease and multiple sclerosis^{12–15}, thus providing proof of concept that CSF derived EVs can be used as a source of biomarkers.

There are various methods available for isolation of EVs, including differential centrifugation, precipitation and size-exclusion chromatography (SEC). Different isolation methods have been described in more detail in a review by Sidhom et al.¹⁶. The selection of isolation method is a balance between EV yield and purity, which poses challenges for EV biomarker discovery; optimising purity is likely to enhance test specificity, whilst optimising EV yield is necessary to maximise test sensitivity. Ultrafiltration combined with size-exclusion chromatography (UF-SEC) outperforms the differential centrifugation method and/or commercial precipitation-based kits for EV isolation from cell culture supernatant, and urine in terms of purity^{16–18}. For CSF EVs, UF-SEC has been reported to increase both yield and purity¹⁹. Density gradient ultracentrifugation produces highly pure EV preparations but is time consuming and requires expensive ultracentrifugation facilities that might not be available in all clinical settings²⁰. SEC, on the other hand, is relatively fast and cost-effective, and requires no specialised laboratory

¹Department of Equine and Small Animal Medicine, Faculty of Veterinary Medicine, University of Helsinki, Helsinki, Finland. ²Department of Immunology, University of Oslo and Oslo University Hospital, Oslo, Norway. ³Epilepsia Helsinki, Member of ERN-EpiCARE, Helsinki University Hospital, Helsinki, Finland. ⁴NanoFCM Co., Ltd, Medicity, Nottingham, UK. ⁵Department of Veterinary Medicine, University of Cambridge, Cambridge, UK. ⁶Faculty of Medicine, University of Helsinki, Helsinki, Finland. ⁷These authors jointly supervised this work: Jenni Karttunen and Tarja S. Jokinen. ✉email: petra.kangas@helsinki.fi

equipment¹⁶. However, it is not capable of separating EVs from similarly sized lipoprotein particles, the latter of which are especially abundant in plasma^{21,22}.

CSF derived EVs have not been widely studied to date, likely because of the invasive collection method and limited volume that can be obtained from individual patients, and because it is difficult to acquire samples from healthy control patients. In a survey performed by International society for Extracellular Vesicles (ISEV) Rigor and Standardization Subcommittee in 2019, only 10% of the respondents had used CSF in their EV studies, which was only a few percentages more compared to the previous survey performed in 2015²³. Also, lipoprotein contamination is a problem with CSF samples. ApoA1 and ApoA2 that are present in CSF are suggested to originate from plasma, and ApoE and ApoJ are suggested to be made within the blood–brain-barrier²⁴. In addition, small quantities of plasma proteins, such as albumin, are present in CSF⁷ and can cause contamination.

Canine spontaneous diseases are utilised in translational research and therefore studying canine CSF can be beneficial also for human studies. In dogs, limited amounts of CSF can be collected (recommended 1 ml maximum per 5 kg body weight), especially from small individuals²⁵. Hence, more information about the minimum CSF starting volume for isolation of a sufficient amount of EVs is needed. Compared to humans, it is easier to collect high volumes of fresh CSF from deceased animals, which enables methodological studies.

Our overall objective was to validate the UF-SEC method for isolation of CSF derived EVs and to determine the minimum CSF volume required for EV proteomic analysis. We first performed a literature review to investigate the current state of CSF EV research, which revealed a need for basic characterisation of EVs. Secondly, we used the UF-SEC method for EV isolation from canine CSF and used a variety of techniques to confirm the presence of EVs and characterise CSF derived EVs. Finally, we compared the EV proteomes obtained from different volumes of CSF in order to find the minimum volume needed for successful proteomic analysis from CSF EVs. Our results indicate that the UF-SEC protocol can be used to isolate purified EVs from CSF, and that a sufficient amount of EVs can be isolated from 0.5 ml of CSF to permit EV proteomic analysis. To our knowledge, this is the first article describing EV isolation from canine CSF.

Results

Literature review. At first, we performed a literature review to investigate the present state of EV analysis from CSF samples. A total of 123 articles were included in the review (Supplementary file S1). Of these, 105 (85%) studies used human CSF for studying the EVs whereas 16 (13%) studies used rodent CSF and 5 (4%) studies used CSF from other species such as pigs, sheep, and horses. In three (2%) of these articles both human and mouse CSF EVs were studied. The highest number of articles ($n = 38$, 31% of total) focused on neurodegenerative diseases (NGD) such as Parkinson's disease or Alzheimer's disease (Fig. 1a). The second highest group comprised articles related to immune-mediated demyelinating diseases (IMDDG), covering a total of 13 (11%) articles. Articles in this group included conditions such as multiple sclerosis or Guillain-Barré syndrome. Articles focusing on EV methodologies also formed a substantial set of 26 articles (21%). The 'other' group included other individual conditions, such as encephalitis, drug abuse, and exercise induced neuroprotection among others ($n = 19$, 15%) (Fig. 1a). Regarding the target of the analysis, most studies investigated EV protein content ($n = 53$, 43%) either by analysing individual proteins ($n = 35$, 28%) or with wider proteomic analysis ($n = 18$, 15%). RNA content was studied in 48 articles (39%) and 18 articles (15%) focused on basic characterisation of EVs, including for example nanoparticle tracking analysis (NTA) or Western blot analysis. Only a few articles studied the biological function of CSF EVs ($n = 2$, 2%) or lipidomics ($n = 2$, 2%) (Fig. 1b).

Next, we reviewed the EV isolation and characterisation methods used in the articles and the volume of CSF from which EVs were derived. The highest number of studies ($n = 37$, 30%) isolated EVs from 1 to 6 ml of CSF, whereas 31 articles (25%) used starting volumes under 1 ml. Unfortunately, a large number of studies (32 articles, 26%) did not report the starting volume (Fig. 1c). Also, 12 articles (10%) did not use specific EV isolation methods despite studying EVs; in these, EVs were analysed directly from the CSF. Two isolation methods were used more often than the others: differential centrifugation-based methods in 49 articles (40%) and precipitation-based methods in 39 articles (32%) (Fig. 1d). SEC-based methods were used in 15 articles (12%). Regarding the basic EV characterisation, the most commonly used methods were electron microscopy (EM) based techniques, Western blot, and NTA, which were used in 61 (50%), 53 (43%) and 48 (39%) articles, respectively (Fig. 1e). Most studies (56 articles, 46%) used one or two different methods to characterise the isolated EVs. In 41 articles (33%) three or more characterisation methods were used, however in 26 studies (21%) specific EV characterisation was not performed (Fig. 1f).

A more detailed technical comparison was performed for the 18 articles which included proteomic analysis from CSF EVs (Supplementary table S1 with full references in Supplementary file S1). A variety of EV isolation methods were used in these studies including differential centrifugation ($n = 4$), precipitation-based methods ($n = 6$) and SEC-based purification ($n = 6$). The starting volume of CSF varied between 8 ml and 50 μ l, but this did not clearly correlate with the number of proteins identified. Most of the articles used pooled CSF for analysis and only five articles analysed more than three biological replicates per group. Mass-spectrometry was the most commonly used technique, although commercial arrays (SOMAscan® array, PEA assay) were used in some articles.

Although SEC was used in a quite small number of CSF EV studies, it is an established isolation method for many biofluids creating relatively pure EV preparations while being accessible for many laboratories¹⁶. Therefore, it was chosen as the isolation method for our canine CSF study.

Sample characteristics. Samples from 21 dogs were included in this study. All but one dog had a CSF nucleated cell count of < 5 cells/ μ l, and one sample had 10 cells/ μ l. All the CSF samples had a protein concentration within the reference interval (< 300 mg/l). Five separate CSF pools were used in the study, two for the method set-up and three for the proteomics analysis.

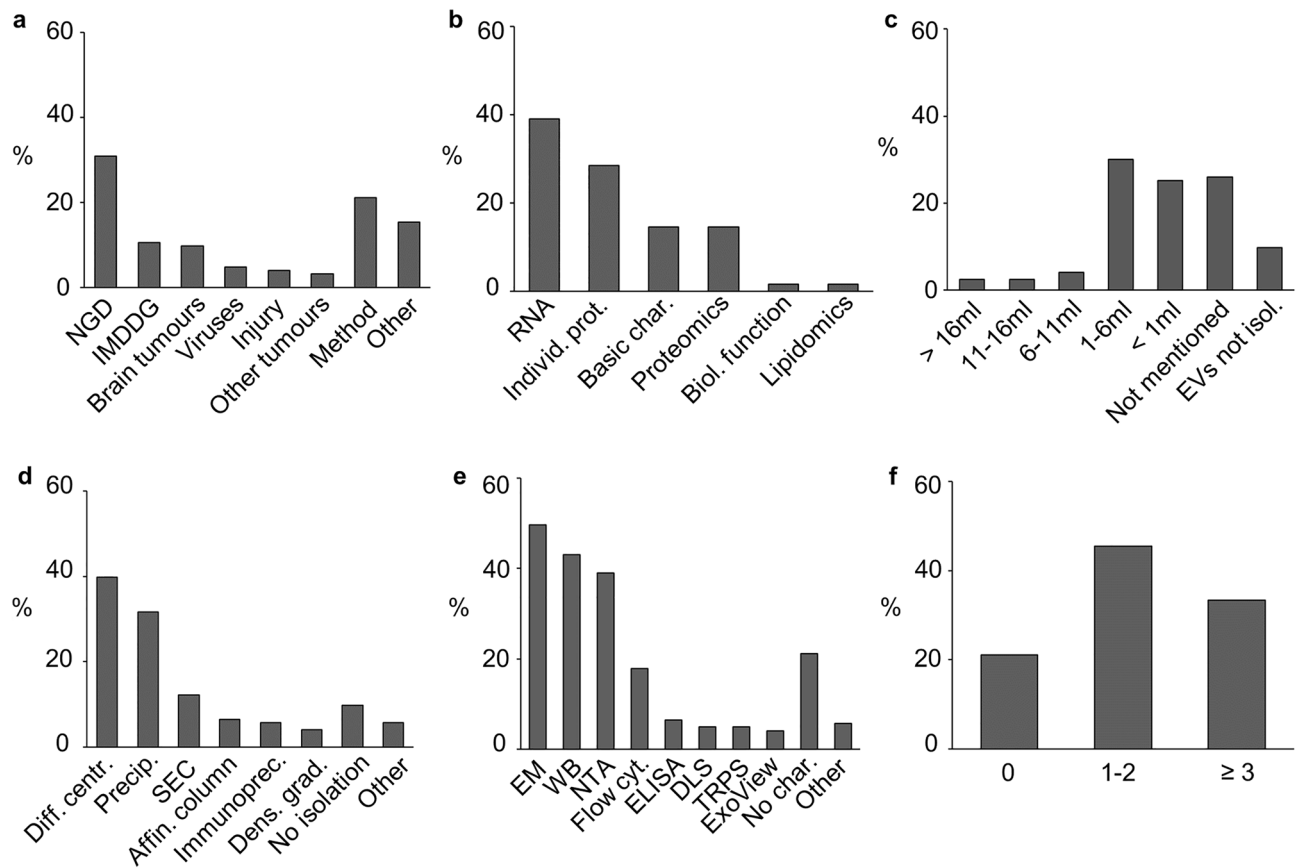


Figure 1. Data from the literature review of CSF EV articles published from 2015 to 2022. **(a)** Conditions studied in the CSF EV articles included in this literature review. **(b)** Targets of the CSF EV analyses. **(c)** The starting volumes used prior to isolation of EVs. **(d)** The isolation methods used. **(e)** The EV characterisation methods used in the studies. **(f)** Number of different characterisation methods used in the articles. CSF = cerebrospinal fluid, EV = extracellular vesicle, NGD = neurodegenerative disease, IMDDG = immune-mediated demyelinating disease group, Individ. prot. = individual proteins, Basic char. = basic characterisation, Biol. function = biological function, EVs not isol. = EVs not isolated, Diff. centr. = differential centrifugation, Precip. = precipitation, SEC = size-exclusion chromatography, Affin. column = affinity column, Immunoprec. = immunoprecipitation, Dens. grad. = density gradient, EM = electron microscopy, WB = Western blot, NTA = nanoparticle tracking analysis, Flow cyt. = flow cytometry, ELISA = Enzyme-Linked Immunosorbent Assay, DLS = dynamic light scattering, TRPS = tunable resistive pulse sensing, No char. = no characterisation.

Extracellular vesicle isolation and characterisation from canine cerebrospinal fluid. The EV characterisation was done with EVs derived from two separate 7 ml pools of CSF. The highest number of particles (determined by NTA) was detected in fraction 3, as expected (Fig. 2a). Protein concentration was highest in fractions 6–8 which was distinct from the particle peak (Fig. 2a). The amount of protein in fractions 3 and 4 was under the detection threshold of the bicinchoninic acid (BCA) assay making it impossible to count particles to protein ratio. Also, Western blot analysis was not sensitive enough to show the presence of canonical EV proteins (data not shown). Later, the presence of several common EV markers was confirmed with the proteomic analysis. Western blot analysis was performed as a purity control for two common EV-contamination proteins in CSF: albumin and ApoA1, a marker of high-density lipoproteins (HDL). Both of these proteins were present mainly in the protein fractions 6–7, confirming relatively good separation from the EVs (Fig. 2b).

The size distribution of the particles was measured with NTA and by nano-flow cytometry (NanoFCM). In general, NanoFCM showed a smaller particle diameter with a narrower particle size distribution compared to NTA. The particles in fraction 3 had a modal size of around 100 nm when measured with NTA and around 70 nm with NanoFCM. The measured particle size slightly decreased in fractions 4 and 5 with both analysis methods as the main peak moved towards smaller particles (Fig. 2c). Raw data of both NTA and NanoFCM measurements is presented in Supplementary figure S5.

Fractions 3–5 were further characterised with TEM and all of them had distinct particle populations. Fraction 3 included cup-shaped particles, a morphology commonly described for EVs²⁶ (Fig. 2d). The particle size was similar to NTA and NanoFCM data. Fraction 4 contained a main population of particles with a diameter of < 50 nm and fraction 5 even smaller particles, with a morphology resembling that of HDL²⁶ (Fig. 2d). Interestingly, most of the particles detected in fractions 4 and 5 were under the detection limit of NTA (70 nm) and

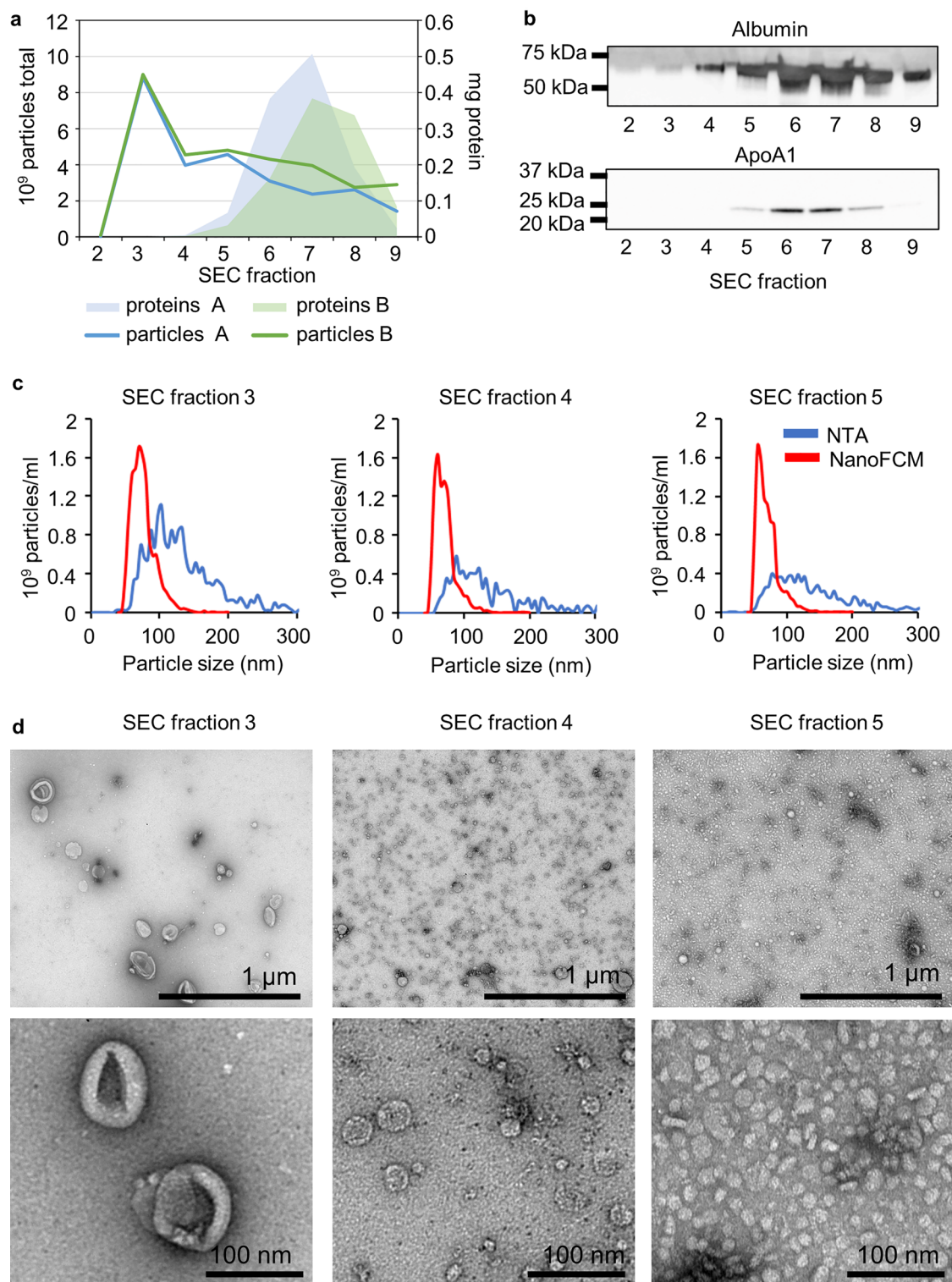


Figure 2. EV characterisation using UF-SEC. (a) Total particle number measured with NTA and protein amount from SEC fractions 2–9 (each 500 μl) from two separate CSF pools (pools A and B). (b) Western blot analysis of albumin and ApoA1 from SEC fractions 2–9 from pool A. The displayed blots are cropped. The uncropped blots can be viewed in Supplementary figure S4. (c) Particle size distribution measured with NTA and NanoFCM from SEC fractions 3–5 of pool B. (d) TEM images from SEC fractions 3–5 from pool B. EV = extracellular vesicle, UF-SEC = ultrafiltration combined with size-exclusion chromatography, CSF = cerebrospinal fluid, NTA = nanoparticle tracking analysis, NanoFCM = nano-flow cytometry, TEM = transmission electron microscopy.

NanoFCM (45 nm with scatter detection). In accordance with BCA assay results, fraction 5 included a darker cloud-like background considered most likely to reflect proteins.

Proteomics comparison of size-exclusion chromatography fractions and cerebrospinal fluid. To further explore differences between the alleged EV fraction and the later SEC fractions, we compared the proteome of SEC fractions 3–5. The workflow for the proteomic analysis is illustrated in Fig. 3. For identification, the LC–MS/MS data was analysed with MaxQuant search engine with and without ‘match between run (MBR)’ active. MBR increases the number of identifications for low-abundant proteins in the samples²⁷. We identified the highest number of proteins from fraction 3 (1493 ± 107 and 999 ± 173 proteins identified with and without MBR, respectively) and lowest number from whole CSF samples (1121 ± 219 and 624 ± 149 proteins identified with and without MBR, respectively) (Fig. 4a, Supplementary table S2 and S3).

For the further comparisons, protein identification results using MBR were used. For each group (fractions 3–5, CSF, CSF depl.), a list of core proteins found in all three replicates was generated (Supplementary figure S1). When these core lists were compared with each other, 537 proteins were shared between all groups, and the highest number of unique proteins ($n=211$) was found from the EV-containing fraction 3, including four proteins (CDC42, RAB5C, RAB10, and RAN) from the Vesiclepedia top 100 list (Fig. 4b). In CSF and CSF depl. combined, 73 proteins that were not present in the SEC fractions were identified. Also, 183 proteins that were not present in fraction 3 were identified in these two groups combined (Fig. 4b).

Heatmap clustering performed for all identified proteins clustered samples from individual SEC fractions together and showed fraction-specific protein clusters (Supplementary figure S2a). Especially fraction 3 included several clusters that were not abundant in other groups. In addition, the proteins unique for the different SEC fractions were compared with cellular component analysis using FunRich. Components considered significantly enriched in fraction 3 were exosomes, lysosome, and cytoplasm. Significantly enriched components for fraction 5 were endoplasmic reticulum and lysosome. No components were considered significant for fraction 4 (Supplementary figure S2b).

Next, Gene set enrichment analysis (GSEA) was used to probe the presence of EV and non-vesicular nanoparticle-related proteins in each fraction. In general, ranked lists for GSEA from all the samples identified ApoA1, ApoE and ApoJ (Clusterin) among the 6 highest ranked proteins, in other words they had high intensities. In addition, albumin was among the top 4 proteins in other groups apart from fraction 4, where it was ranked as the 11th most abundant protein. Using Vesiclepedia top 100 proteins as a protein list, the greatest positive enrichment for EV associated proteins was detected within fraction 3 with a nominal p -value of < 0.001 (Fig. 4c). Fraction 4 was also enriched with EV associated proteins with a nominal p -value of 0.017, but with higher false discovery rate, indicating lower enrichment compared to fraction 3. Even though a relatively similar number of Vesiclepedia top 100 proteins was present in fraction 5 and whole CSF samples, they were not significantly enriched, and EV-related proteins had low relative intensity compared to other proteins in the samples (Fig. 4c). Separate protein lists were generated for exomeres and supermeres, recently reported non-vesicular nanoparticles with the size range present in TEM images from fractions 4 and 5^{1,3,4}. With these lists, only enrichment detected was in fraction 3 using the supermere list. No enrichment was detected for the exomere list (Supplementary figure S2c). Protein lists used in the GSEA are available in Supplementary table S4.

As a final analysis, we compared the mean normalised Intensity Based Absolute Quantification (iBAQ) values from selected individual proteins from SEC fractions 3–5 (Fig. 4d). First group was apolipoproteins involved in the structures of HDL, low-density lipoproteins (LDL), chylomicrons, and ApoJ (Clusterin) which is connected to several neurodegenerative diseases^{28,29}. All apolipoproteins had highest intensities in fractions 4 and

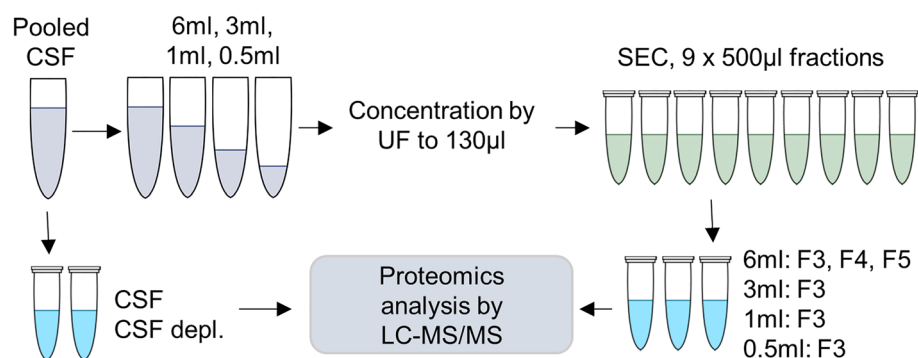


Figure 3. Workflow of the proteomic analysis. Pooled CSF was divided into a whole CSF sample with and without depletion, and into four different starting volumes (6 ml, 3 ml, 1 ml, and 0.5 ml). An UF–SEC protocol was used to fractionate the samples of the different volumes. At first, the CSF samples and fractions 3–5 from the 6 ml starting volume were analysed and compared to evaluate the presence of EVs. In second comparison, the effect of CSF starting volume for EV protein contents was studied by comparing the fraction 3 of the four different starting volumes. UF–SEC = ultrafiltration combined with size-exclusion chromatography, CSF: cerebrospinal fluid, EV = extracellular vesicle, CSF depl. = CSF with depletion of highest abundant plasma proteins, LC–MS/MS = liquid chromatography with tandem mass spectrometry.

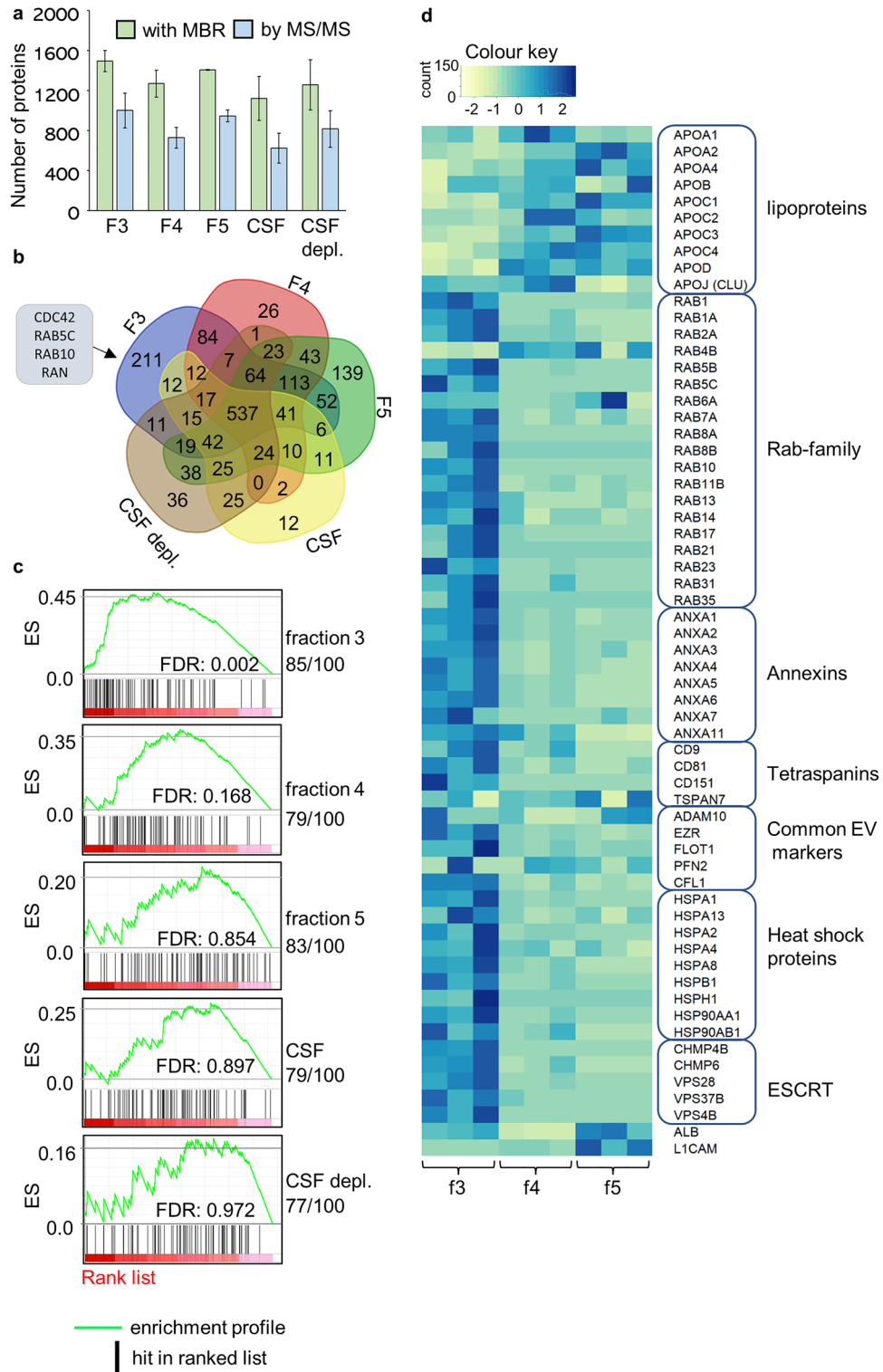


Figure 4. Proteomics comparison of SEC fractions and CSF. **(a)** The number of identified proteins in the SEC fractions 3–5 isolated from 6 ml of CSF, plain CSF and CSF depl. Protein number was calculated with and without the MBR setting. The values are given in mean and SD of three replicates. **(b)** A Venn diagram from core protein list (found from each 3 rounds) of each fraction and CSF samples. Four proteins unique for fraction 3 aligning with the Vesiclepedia top 100 are listed. **(c)** GSEA performed with the Vesiclepedia top 100 protein list. The number of proteins found from each rank list is given under the sample name. The ranked protein list was generated from the proteomics intensity data and is expressed in red in the plot, darker colour representing higher intensity. Black lines represent a protein included in the protein list and enrichment score represents the level of enrichment. **(d)** Heatmap without clustering performed from iBAQ data for selected EV-related proteins from each fraction. Color key shows Row z-score of normalised counts. CSF = cerebrospinal fluid, CSF depl. = CSF with depletion of highest abundant plasma proteins, MBR = matches between runs, SD = standard deviation, GSEA = Gene set enrichment analysis, iBAQ = Based Absolute Quantification, ES = enrichment profile, FDR = false recovery rate.

5, indicating a presence of lipoprotein particles. To further explore EV related proteins, we used a general EV marker listing prepared by Crescitelli et al. (Table 1 in their article)³⁰. Apart from individual proteins (RAB4B, TSPAN7), the highest intensity was consistently detected in fraction 3. Lastly, albumin and L1-CAM were also added to the list as they are considered relevant regarding CSF EVs^{2,31,32}, both of which had highest intensity in fraction 5, likely reflecting the presence of non-vesicular proteins.

Comparison of cerebrospinal fluid starting volume. In addition to fraction comparison from 6 ml of pooled CSF, UF-SEC isolation was performed from 3 ml, 1 ml and 0.5 ml of each CSF pool. For those samples, proteomic analysis of fraction 3 was performed to compare the effect of starting volume on EV yield and number of proteins identified in the EV enriched fraction.

As expected, the highest total number of particles was found from the 6 ml starting volume ($10.6 \times 10^9 \pm 3.4 \times 10^9$ particles) and the lowest in the 0.5 ml starting volume ($4.7 \times 10^8 \pm 1.7 \times 10^8$ particles) (Fig. 5a). When particle number was normalised per 1 ml of CSF used, the highest particle number was again found from the 6 ml samples indicating a higher recovery of EVs from larger volumes compared to lower volumes. With the other starting volumes, the differences in EV recovery varied between rounds indicating no clear differences based on starting volume used (Fig. 5b).

For the total number of proteins, the proteomics data was again analysed separately using both the MBR and 'by MS-MS' methods. With all samples, MBR analysis identified a higher number of proteins, with the highest

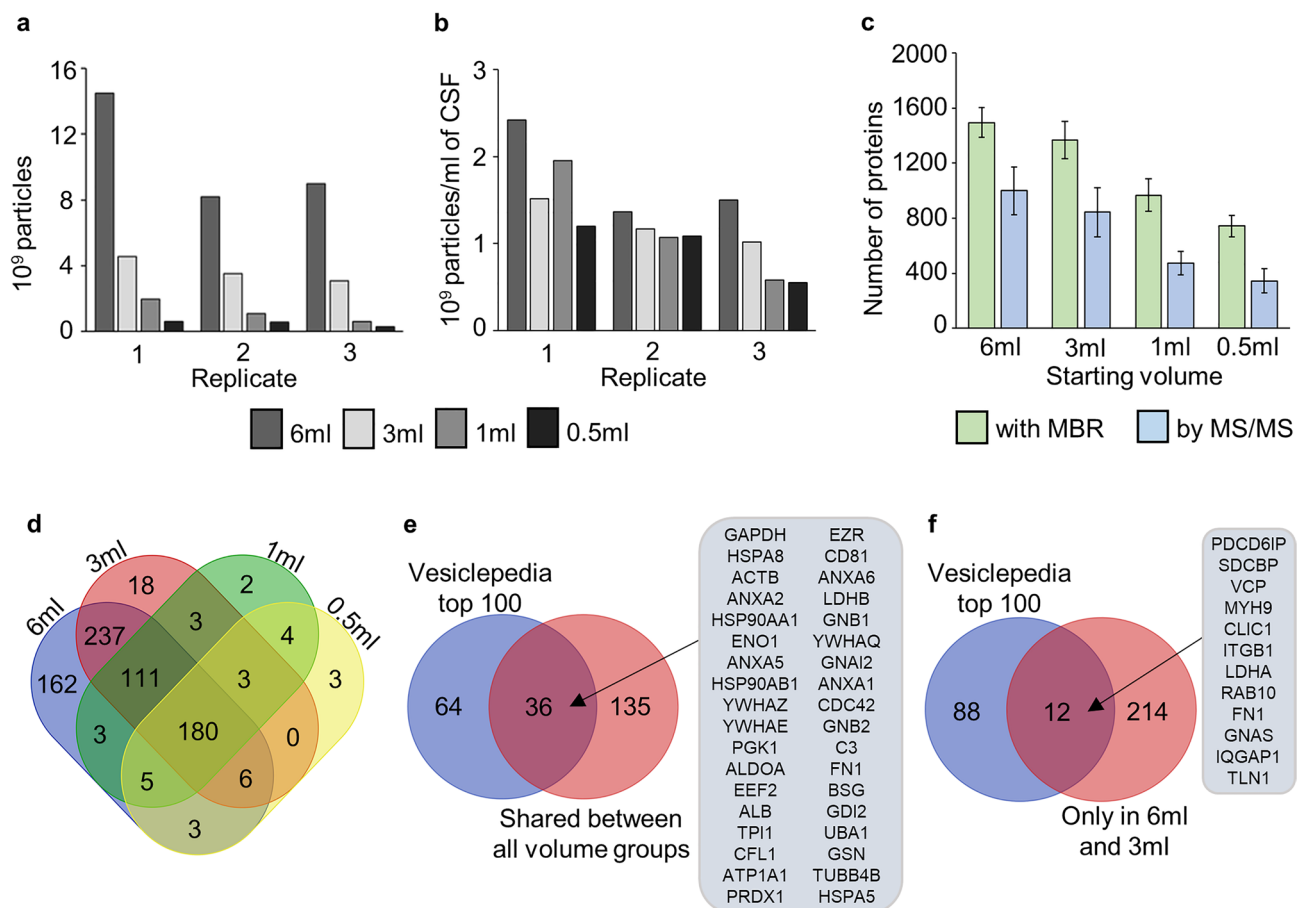


Figure 5. Comparison of CSF starting volume. (a) The total number of particles in the EV fraction of each starting volume measured with NTA. (b) The particle count per 1 ml of CSF in the EV fraction of each starting volume. (c) Total number of proteins identified from each starting volume's EV fraction. The result is given as a mean and SD between all three replicates. (d) A Venn diagram of the shared proteins between the different starting volumes' EV fractions. Proteins identified in every replicate for each starting volume were included in the analysis. (e) Alignment with the Vesiclepedia top 100 for the proteins shared between the EV fractions of all the starting volumes. Only proteins with corresponding gene names available were used for the analysis. The proteins aligning with Vesiclepedia are listed in the figure. (f) Alignment with the Vesiclepedia top 100 for the proteins shared between the EV fractions of 6 ml and 3 ml starting volumes that were not identified in the 1 ml or 0.5 ml starting volumes. Only proteins with corresponding gene names available were used for the analysis. The proteins aligning with the Vesiclepedia top 100 are listed in the figure. CSF = cerebrospinal fluid, EV = extracellular vesicle, NTA = nanoparticle tracking analysis, SD = standard deviation, MBR = matches between runs.

number of proteins identified from the 6 ml starting volume (1493 ± 107 or 999 ± 173 proteins) and the lowest number of proteins identified in the 0.5 ml starting volume (743 ± 77 or 345 ± 88 proteins) (Fig. 5c).

Further comparison of the starting volumes was done without MBR, as we were interested in finding out if the proteomic analysis can in the future be conducted on individual dogs without a large sample series. First, core lists of proteins derived from EVs isolated from different volumes of CSF were generated by listing all the proteins present in each proteomics replicate (Supplementary figure S3a). A Venn diagram of these core lists shows a total of 180 proteins present in all the volume groups (Fig. 5d). For 171 of these, a gene name could be found (Supplementary table S5). Of these 171 proteins, 36 were included in the Vesiclepedia top 100 list (Fig. 5e). In addition to the proteins shared between all the volume groups, the 6 ml and 3 ml volumes shared 237 proteins that were not present in the smaller volumes (Fig. 5d, Supplementary figure S3b). Gene names were found for 226 of these, and 12 aligned with the Vesiclepedia top 100 (Fig. 5f). A list of unique gene names of proteins identified in all three proteomics replicates in the 6 ml starting volume is presented in Supplementary table S6, forming a list of stable EV related proteins in canine CSF.

Discussion

Here, our aim was to validate the UF-SEC method for isolation of EVs from canine CSF and to determine the smallest possible starting volume for reliable EV proteomic analysis. We mapped out the state of current CSF EV research and continued by comparing different SEC fractions and starting volumes of CSF.

The literature review revealed a high variability in the methods used and rigour in articles studying CSF EVs and that the reproducible information of EVs in CSF is still sparse. A large variety of different conditions has been studied, proving the potential for studying brain-related diseases. SEC is an increasingly popular technique for isolating the CSF EVs, however differential centrifugation or precipitation -based EV purification was used in over 70% of the articles, even though they are not optimal regarding the purity of vesicles^{33,34}. A variety of characterisation methods were used throughout the articles although electron microscopy, Western blot, and NTA were the most common. The majority of the articles characterised the EV preparations only with a maximum of two methods, and hence not fulfilling the MISEV guidelines². Furthermore, 10% of articles did not perform EV isolation and 21% did not characterise the EVs at all. This could be because collecting CSF is an invasive procedure and the volumes obtained are small, limiting the material available for basic characterisation. Thus, there is still a need for basic characterisation of CSF EVs and for the MISEV 2018 guidelines² to be followed more closely.

In our study, NTA measurement showed a clear particle peak at SEC fraction 3, which is consistent with findings when EVs are isolated from other body fluids using the same method¹⁸. In fraction 3, particles detected by NTA had a modal size of around 100 nm, whereas particles measured by NanoFCM had a modal size of around 70 nm. Differences between the techniques detected in our study are consistent with previous findings³⁵. Characterisation by TEM and proteomic analysis was then used to prove that the SEC fraction 3 is, in fact, enriched with EVs. In this study, we were not able to perform immunoblotting of EV markers and opted to prove their existence with the proteomic analysis instead. It is challenging to find working antibodies for dogs and especially ones that would be sensitive enough to work on lower abundant proteins in CSF EVs. Still, mass spectrometry is a valid way of assessing the presence of EV markers, and several markers could be found in our analysis^{2,36}.

Interestingly, TEM imaging also revealed distinct particle populations in fractions 4 and 5, with fraction 5 morphology resembling that of HDL²⁶. Lipoprotein particles including HDL, LDL, VLDL and chylomicrons are known contaminants in EV preparations in plasma and they may co-isolate with EVs using SEC-based methods^{21,22}. In addition, new types of smaller non-membranous extracellular particles have been discovered in recent years, including exomeres and supermeres^{1,3,4}, and it could be hypothesised that these represent the particles seen in fractions 4 and 5. However, our data would not support this hypothesis since all proteins associated with small and large sized EVs (heat shock proteins were enriched in large EVs and tetraspanins, ADAMs, ESCRT proteins, SNAREs and Rab proteins were enriched in small EVs⁶) were found in fraction 3, and enrichment for supermere proteins was only identified in fraction 3. Also, the exomere listing was not enriched in fractions 3–5. Fractions 4 and 5 also had the highest relative intensity of apolipoproteins, supporting the premise that the particles identified in fractions 4 and 5 with TEM were mainly lipoproteins.

Despite separate protein profiles, the most abundant proteins were similar in all the SEC fractions and in whole CSF samples, and the number of shared proteins was high. Fraction 4 was enriched with Vesiclepedia top 100 proteins, but with lower abundance compared to fraction 3, whereas fraction 5 contained more non-vesicular proteins than the earlier SEC fractions. These data indicate that i) fraction 3 includes the majority of EVs, but also small quantities of lipoprotein particles, and ii) a small amount of EVs is present also in the other fractions. Although SEC did not fully fractionate EVs from other components of the CSF, fraction 3 did include the highest number of individual proteins compared to whole CSF, likely representing a reduction in the abundance of contaminant proteins (for example albumin) that might mask the presence of other proteins of lower abundance. Together with the Western blot analysis for ApoA1 and albumin, our proteomics data shows that our UF-SEC protocol was successful in reducing the quantity of non-vesicular proteins and lipoprotein contaminants from the EV fraction, which is in line with previous articles showing successful SEC-based EV isolation from CSF^{19,37,38}.

L1-CAM has traditionally been considered as a marker for neuronal EVs³¹, although it was recently suggested that L1-CAM or its isoforms are not carried by EVs in either human plasma or CSF³². In our study, L1-CAM was identified from the unpurified CSF and from the SEC fractions 4 and 5, and was not consistently identified within fraction 3. These data indicate that L1-CAM might not be strongly associated with EVs in canine CSF, supporting the data from the aforementioned study³².

The previous proteomics studies from CSF EVs have used variable starting volumes and methods for EV isolation, and most used pooled CSF. Pooled samples are useful in methodological comparisons, but in the clinical setting analysis of individual patient samples is usually required, although the limited CSF volume that

can be obtained from patients ante-mortem can be a limiting factor. As expected, both absolute EV yield and the number of proteins identified correlated with the starting volume used. The number of particles varied between the pools showing biological variability. Promisingly, sufficient amount of EVs could be isolated from 0.5 ml of CSF to permit proteomic analysis, with 293–447 proteins identified from such samples without the MBR setting active, thus providing proof of concept that proteomic analysis of EVs could be performed on individual canine patient samples. In addition, when the MaxQuant analysis was performed using the MBR setting, we were able to identify 696–832 proteins from the 0.5 ml samples. This is in line with recent findings of Hirschberg et al., also successfully isolating vesicles from 0.5 ml of CSF and being able to identify a sufficient amount of proteins in the vesicle fraction³⁹. This could be a useful option for further clinical proteomics studies on CSF EVs if it is possible to include one sample with larger starting volume to boost the overall number of identifications. In addition, 180 common proteins were identified in all the replicates of all the four volumes showing reproducibility. In the future, these proteins could further be evaluated with larger study sets.

Despite the challenges, CSF EVs hold high potential for biomarker studies of brain related diseases. There is an ever-growing interest in EV research, but CSF EVs are yet to be studied on a larger scale. Our data suggest that the UF-SEC method effectively enriches EVs and reduces the amount of contaminant proteins present in EV enriched fractions. The NTA and proteomic analysis showed that sufficient EVs can be isolated from 0.5 ml of CSF to permit proteomic analysis, although a volume of ≥ 3 ml of CSF is likely to allow more complete proteomic analysis.

Methods

Literature review. For the literature review, we searched articles about CSF EVs from the following online databases: Web of Science, PubMed, EV Track, Wiley Online Library and Google Scholar using the search term cerebrospinal fluid combined with the terms extracellular vesicles, exosomes, microvesicles, ectosomes and apoptotic bodies. An asterisk was used when necessary to broaden the search results. We only included original research articles published in 2015 or later in the study and the searches were done between April 2021 and August 2022. We reviewed the articles for the starting volume of CSF, for the isolation and characterisation methods, and the number of different characterisation methods used per study. The objectives of the studies were also noted. Articles analysed for the literature review can be found in the Supplementary file S1.

Cerebrospinal fluid collection. Cerebrospinal fluid was collected from dogs euthanised at the Veterinary Teaching Hospital of the University of Helsinki, Finland. The study was approved by the Viikki Campus Research Ethics Committee at the University of Helsinki, Finland and carried out in compliance with the Animal Research: Reporting of In Vivo Experiments (ARRIVE) guidelines. The dogs were euthanised for various reasons unrelated to our study and all the carcasses were donated to teaching and research purposes with written informed consent from the owner. CSF was collected from a total of 21 dogs.

CSF was collected via a cisternal tap with a sterile puncture within one hour of euthanasia. As much CSF as possible was drained from each dog into 2 ml plain tubes. Samples were visually assessed to be clear of any visible red blood cell contamination. Within 30 min of collection, total nucleated cell count (TNCC) and total protein concentration were determined. The TNCC and red blood cell count were determined by directly placing undiluted and well-mixed CSF into a Bürker counting chamber (0,640,210, Paul Marienfeld GmbH & Co. KG, Lauda-Königshofen, Germany). One side of the chamber was filled, and all cells were counted using a Nikon ECLIPSE Ci-L microscope (Nikon, Tokyo, Japan) at 40X magnification. Pleocytosis was defined as TNCCs > 5 cells/ μ l. The remainder of the sample was centrifuged at $4000 \times g$ for 10 min (with brake) at room temperature to pellet any cellular material (Eppendorf 5424, Eppendorf AG, Hamburg, Germany). The supernatant was transferred into a new tube, from where it was divided into Protein LoBind tubes (#022,431,081, Eppendorf AG, Hamburg, Germany), snap-frozen in liquid nitrogen and stored at -80 °C until further use.

Extracellular vesicle isolation. Prior to EV isolation, CSF aliquots were thawed on ice, pooled, and 1/100 volume of protease inhibitor (#P8340, Sigma-Aldrich, St. Louis, Missouri, United States) was added to eliminate any proteases that could destroy the proteins in the samples. The pool was centrifuged at $4000 \times g$ for 20 min at 4 °C to remove any remaining debris. For method set-up, two 7 ml pools of CSF were used. For proteomic analysis, three separate pools of 12 ml were divided into four volumes: 6 ml, 3 ml, 1 ml, and 0.5 ml, which were then processed individually. The individual pools used for the experiments were created by combining CSF from 2 to 8 dogs.

For the UF-SEC isolation of EVs, the samples were first concentrated by centrifugation at $4000 \times g$ at 21 °C using Amicon® Ultra-4 Centrifugal Filter Unit with 100 kDa molecular weight cutoff (UFC810024, Merck Millipore, Burlington, Massachusetts, United States). After sample concentration, the final volume of each sample was adjusted to 130 μ l with PBS. SEC was performed with qEV single/70 nm Legacy columns (SP2, Izon, Christchurch, New Zealand), according to manufacturer's protocol. Briefly, the column was rinsed with a minimum of 10 ml of PBS and 130 μ l of the concentrated sample was loaded into the column. PBS was added as needed and nine 500 μ l fractions were collected.

Before the proteomics comparisons, an aliquot of 50 μ l was taken from each fraction for NTA and BCA analysis and the rest of the fraction was stored at -80 °C prior to proteomic analysis.

Characterisation. *Bicinchoninic acid assay.* The protein concentration of each fraction was measured using the Pierce BCA Protein Assay Kit (#23227, Thermo Scientific™, Waltham, Massachusetts, United States) according to the manufacturer's instructions. Briefly, two sets of standards and 25 μ l of each sample were mixed with 200 μ l of working reagent on a well plate. The plate was incubated at 37 °C for 30 min and read at a wave-

length of 562 nm with the Multiskan GO instrument and the Thermo Scientific SkanIt software (Thermo Scientific™, Waltham, Massachusetts, United States). The BCA assay was done once per sample.

Western blot. Western blot analysis was performed for SEC fractions 2–9. The samples were combined with a self-prepared 10X sample buffer (sodium dodecyl sulfate (4%), tris hydrochloride (0.125 M), glycerol (20%), bromophenol blue (0.006%), 2-mercaptoethanol (10%)) and boiled for 10 min. Of each fraction, 10 µl (for the albumin gel) or 20 µl (for the ApoA1 gel) were loaded into 4–20% Mini-PROTEAN® TGX™ Precast Protein gels (#4561093, Bio-Rad Laboratories, Hercules, California, United States) and run at 200 V for 35 min. The proteins were transferred to nitrocellulose membranes using Power Blotter Select Transfer Stacks (#PB3310, Invitrogen, Waltham, Massachusetts, USA) and semi dry transfer with Power Blotter Station (Invitrogen, Waltham, Massachusetts, USA). Membranes were blocked for 1 h in Tris Buffered Saline with Tween (0.1% Tween-20, #1706531, Bio-Rad Laboratories, Hercules, California, United States) 5% milk (Skimmed milk powder instant, Valio, Helsinki, Finland), and incubated overnight with primary antibodies against albumin (dilution 1:20,000, #ab194215, Abcam, Cambridge, UK) or ApoA1 (dilution 1:3000, #ab227455, Abcam, Cambridge, UK) in the blocking buffer. Membranes were washed three times and incubated with secondary antibodies: Donkey anti Sheep/Goat IgG (dilution 1:100,000, #STAR88P, Bio-Rad Laboratories, Hercules, California, United States), Goat Anti-Rabbit Immunoglobulins/HRP (dilution 1:100,000, #P0448, Dako Denmark A/S, Glostrup, Denmark) for 1 h in room temperature, after which the washing steps were repeated. SuperSignal™ West Atto Ultimate Sensitivity Substrate (#A38554, Thermo Scientific™, Waltham, Massachusetts, United States) was applied on the membranes and the chemiluminescence was detected using FujiFilm LAS-3000 imager.

Nanoparticle tracking analysis. The samples were diluted in ultrapure water and the numbers of particles were measured using ZetaView® PMX120 (Particle Metrix, Meerbusch, Germany). Measurements were done once at all 11 positions and the video quality was set to medium. Lower detection limit was provided by the manufacturer. The dilution factor varied between 50 and 500 depending on the sample. The measured volume was 1 ml and the measurement time 10 s. The chamber temperature was set to 22 °C, and the sensitivity of the camera to 85. Data were analysed using the ZetaView® analysis software version 8.05.12 with a minimum area of 10, a maximum area of 1000 and a minimum brightness of 30.

Nano-flow cytometry. A NanoAnalyzer U30 instrument (NanoFCM Co., Ltd, Nottingham, UK) with a 488 nm laser and single-photon counting avalanche photodiode detectors (SPCM APDs) was used for determination of size and concentration of individual particles using side scattered light through a bandpass filter of 488/10 nm. The gravity-fed sheath fluid system consisted of HPLC grade water, focusing the sample core stream diameter to ~ 1.4 µm. Measurements were taken over 1-min durations at a sampling pressure of 1.0 kPa. Particle concentrations were determined against a standard of 250 nm silica nanoparticles of known concentration. For particle sizing, a standard consisting of a 4-modal silica nanosphere cocktail (NanoFCM Inc., S16M-Exo) with diameters of 68, 91, 113 and 155 nm was used. Lower detection limit was provided by the manufacturer. Each sample was measured once for size and concentration. Between 4000 and 7000 events were recorded for each sample. Flow rate was 50.71 nL/min. Triggering was done via side scatter channel (SS-H). Thresholding is performed by the analysis software to be set at three standard deviations and the mean of the background, with only events above this threshold being plotted as true particle events.

For assay controls, the Tris–EDTA buffer used as the diluent was analysed separately. This was then used as a blank, whereby the number of events in the blank and their size profile was removed from final sample results. The instrument was calibrated using 250 nm SiNP QC beads (NanoFCM Co., Ltd, Nottingham, UK) that fluorescence in both FITC and APC range. The intensity of this fluorescence as well as the side scatter intensity of the 250 nm particles were used to align the lasers and detectors to optimum detection resolution and sensitivity within the software. These beads were of a known concentration (2.37E10 particles/ml), thus providing the concentration standard for the samples to be compared against. For size calibration four silica nanospheres of known sizes (68 nm, 91 nm, 113 nm and 155 nm) in a cocktail are analysed and the 4 distinct peaks mapped by the software to create a standard curve relating intensity of side scatter to the size in nm of the particles, providing the basis for sizing of the samples.

A standard curve was generated based on the side scattering intensity of the four different silica particle sub-populations using the NanoAnalyzer software. The laser was set to 10mW and 10% side scatter decay. Data processing and analysis was performed using the NanoFCM Professional Suite v2.0 software.

Transmission electron microscopy. The grids used were 200 square Mesh copper 3.05 mm (G2200C, Agar Scientific, Stansted, UK). The film was made by hand in 2% biofoam in chloroform solution (SPI-Chem™ Pioloform® Resin, #2466, SPI Supplies, West Chester, PA, USA). Carbon coating was done with Bal-Tec CED030 carbon thread evaporator (Bal-Tec Union Ltd., Liechtenstein) and Emitech K100X Glow discharge unit (Emitech Ltd., UK) was used as the glow discharge system. Grids were then placed on a 10 µl droplet of sample on parafilm for 2 min. Buffer salts were removed by transferring the grids twice to a fresh drop of distilled water and incubated for 5 s each. The excess fluid was removed with filter paper and the grids were transferred to one drop of uranyl acetate (1.5% in distilled water) and incubated for 1 min. Excess fluid was removed with filter paper and the grids were air dried prior to imaging. The samples were imaged using a Jeol JEM-1400 transmission electron microscope with 80,000 V and magnifications of 6000X and 20,000X.

Proteomics. EV samples (~ 450 µl) were lysed, proteins precipitated and digested into peptides with trypsin using a previously published protocol for protein aggregation capture⁴⁰. First, acetonitrile (ACN) was added to

EV samples so that the final ACN concentration was 70%, proteins were precipitated using MagReSynAmine beads (ReSyn Biosciences), captured with magnetic rack and washed with 100% ACN and 70% ethanol. Then 50 mM NH_4HCO_3 was added to the beads, and proteins were reduced with DTT, alkylated with iodoacetic acid and on-beads digested with trypsin (Promega) over night. In addition to fraction 3 (from 6 ml, 3 ml, 1 ml, 0.5 ml of CSF) and SEC fractions 4–5 (obtained from 6 ml of CSF), also intact and depleted CSF samples were analysed with liquid chromatography with tandem mass spectrometry (LC–MS/MS). Intact CSF samples were prepared using the same protocol used with EVs. For depletion of the most abundant proteins from CSF ProteoSpin Abundant Serum Protein depletion kit (Norgen Biotek) was used according to manufacturer's instructions, and proteins were in-solution digested with trypsin after depletion.

The resulting tryptic peptides were purified using home-made C18 Stage tips-columns followed by nanoLC-MS/MS analysis with nanoElute coupled to timsTOF fleX (Bruker). Peptide separation was done using 60-min linear separation gradient with 0–35% ACN using 25 cm Aurora C18 column (Ion Optics). The timsTOF fleX was operated in PASEF mode. Mass spectra for MS and MS/MS scans were recorded between m/z 100 and 1700. Ion mobility resolution was set to 0.60–1.60 $\text{V}\cdot\text{s}/\text{cm}$ over a ramp time of 100 ms. Data-dependent acquisition was performed using 10 PASEF MS/MS scans per cycle with a near 100% duty cycle. A polygon filter was applied in the m/z and ion mobility space to exclude low m/z , singly charged ions from PASEF precursor selection. An active exclusion time of 0.4 min was applied to precursors that reached 20 000 intensity units. Collisional energy was ramped stepwise as a function of ion mobility.

For protein identification the data from LC–MS/MS was analysed by MaxQuant ver 2.0.1.0 against dog (*Canis lupus*) database downloaded from Uniprot in November 2021. MaxQuant searches were done with and without 'match between runs' active. The searches were done using MaxQuant's default parameters with a false discovery rate of 1% on protein and peptide level.

Data analysis. In the proteomics data analysis, two different methods of identifying proteins were used: identification by LC–MS and identification by matching to a library created from all the analysed samples. For Venn diagrams, an online tool from Bioinformatics Institute Ghent was used (<https://bioinformatics.psb.ugent.be/webtools/Venn/>). Pathway analysis was done with FunRich version 3.1.4, with the level of significance set on $p \leq 0.05$.

GSEA was performed with GSEA 4.1.0 program using 'GSEApreranked' option. A rank list was generated for each sample by giving the lowest rank number for protein with highest total intensity. After this an average of the ranks of three replicate samples was calculated and the final group rank list was generated based on that. Protein list for Vesiclepedia top 100 proteins was taken from its website on June 14th 2022. Protein list for exomeres was generated from differential expression data between small EVs and distinct nanoparticles from Zhang et al. 2019, proteins with positive logFC and adjusted p -value < 0.05 were selected⁴. Out of the 103 proteins, 58 were identified from the proteomics data and were used as the protein list. Supermere protein list was generated by combining the top 20 most abundant proteins in supermeres derived from three cell lines presented in Supplementary Table 4³. Out of the 34 proteins, 28 identified from the proteomics data were used as the protein list.

Proteomic and NTA data are presented as mean \pm standard deviation unless otherwise stated.

Data availability

The proteomics data are available via ProteomeXchange with identifier PXD036748.

Received: 20 December 2022; Accepted: 8 June 2023

Published online: 12 June 2023

References

- Crescitelli, R. *et al.* Subpopulations of extracellular vesicles from human metastatic melanoma tissue identified by quantitative proteomics after optimized isolation. *J. Extracell. Vesicles* **9**, 1722433 (2020).
- Théry, C. *et al.* Minimal information for studies of extracellular vesicles 2018 (MISEV2018): A position statement of the International Society for Extracellular Vesicles and update of the MISEV2014 guidelines. *J. Extracell. Vesicles* **7**, 1535750 (2018).
- Zhang, Q. *et al.* Supermeres are functional extracellular nanoparticles replete with disease biomarkers and therapeutic targets. *Nat. Cell. Biol.* **23**, 1240–1254 (2021).
- Zhang, Q. *et al.* Transfer of functional cargo in exomeres. *Cell Rep.* **27**, 940–954.e6 (2019).
- Zhang, H. *et al.* Identification of distinct nanoparticles and subsets of extracellular vesicles by asymmetric flow field-flow fractionation. *Nat. Cell. Biol.* **20**, 332–343 (2018).
- Lischinig, A., Bergqvist, M., Ochiya, T. & Lässer, C. Quantitative proteomics identifies proteins enriched in large and small extracellular vesicles. *Mol. Cell. Proteomics* <https://doi.org/10.1016/j.mcpro.2022.100273> (2022).
- Spector, R., Robert Snodgrass, S. & Johanson, C. E. A balanced view of the cerebrospinal fluid composition and functions: Focus on adult humans. *Exp. Neurol.* **273**, 57–68 (2015).
- Sturges, B. K. Cerebrospinal Fluid Sampling. in *Small Animal Critical Care Medicine* 1064–1068 (Elsevier, 2015). doi:<https://doi.org/10.1016/B978-1-4557-0306-7.00207-5>.
- Sakka, L., Coll, G. & Chazal, J. Anatomy and physiology of cerebrospinal fluid. *Eur. Ann. Otorhinolaryngol. Head Neck Dis.* **128**, 309–316 (2011).
- Upadhyay, R. & Shetty, A. K. Extracellular vesicles for the diagnosis and treatment of Parkinson's disease. *Aging Dis.* **12**, 1438 (2021).
- Chiasserini, D. *et al.* Proteomic analysis of cerebrospinal fluid extracellular vesicles: A comprehensive dataset. *J. Proteomics* **106**, 191–204 (2014).
- Sandau, U. S. *et al.* Differential effects of APOE genotype on MicroRNA cargo of cerebrospinal fluid extracellular vesicles in females with Alzheimer's disease compared to males. *Front. Cell Dev. Biol.* **10**, 864022 (2022).
- Gelibter, S. *et al.* Spinal fluid myeloid microvesicles predict disease course in multiple sclerosis. *Ann. Neurol.* **90**, 253–265 (2021).
- Muraoka, S. *et al.* Proteomic profiling of extracellular vesicles derived from cerebrospinal fluid of Alzheimer's disease patients: A pilot study. *Cells* **9**, 1959 (2020).

15. Geraci, F. *et al.* Differences in intercellular communication during clinical relapse and gadolinium-enhanced MRI in patients with relapsing remitting multiple sclerosis: A study of the composition of extracellular vesicles in cerebrospinal fluid. *Front. Cell. Neurosci.* **12**, 418 (2018).
16. Sidhom, K., Obi, P. O. & Saleem, A. A review of exosomal isolation methods: Is size exclusion chromatography the best option?. *IJMS* **21**, 6466 (2020).
17. Allelein, S. *et al.* Potential and challenges of specifically isolating extracellular vesicles from heterogeneous populations. *Sci. Rep.* **11**, 11585 (2021).
18. Karttunen, J. *et al.* Size-exclusion chromatography separation reveals that vesicular and non-vesicular small RNA profiles differ in cell free urine. *IJMS* **22**, 4881 (2021).
19. Thompson, A. G. *et al.* UFLC-derived CSF extracellular vesicle origin and proteome. *Proteomics* <https://doi.org/10.1002/pmic.201800257> (2018).
20. Ayala-Mar, S., Donoso-Quezada, J., Gallo-Villanueva, R. C., Perez-Gonzalez, V. H. & González-Valdez, J. Recent advances and challenges in the recovery and purification of cellular exosomes. *Electrophoresis* **40**, 3036–3049 (2019).
21. Karimi, N. *et al.* Detailed analysis of the plasma extracellular vesicle proteome after separation from lipoproteins. *Cell. Mol. Life Sci.* **75**, 2873–2886 (2018).
22. Simonsen, J. B. What are we looking at? Extracellular vesicles, lipoproteins, or both?. *Circ. Res.* **121**, 920–922 (2017).
23. Royo, F., Théry, C., Falcón-Pérez, J. M., Nieuwland, R. & Witwer, K. W. Methods for separation and characterization of extracellular vesicles: Results of a worldwide survey performed by the isev rigor and standardization subcommittee. *Cells* **9**, 1955 (2020).
24. Ladu, M. J. *et al.* Lipoproteins in the central nervous system. *Ann. N.Y. Acad. Sci.* **903**, 167–175 (2000).
25. Di Terlizzi, R. & Platt, S. R. The function, composition and analysis of cerebrospinal fluid in companion animals: Part II – Analysis. *Vet. J.* **180**, 15–32 (2009).
26. Lauer, M. E. *et al.* Cholesteryl ester transfer between lipoproteins does not require a ternary tunnel complex with CETP. *J. Struct. Biol.* **194**, 191–198 (2016).
27. Prianchnikov, N. *et al.* MaxQuant software for ion mobility enhanced shotgun proteomics. *Mol. Cell. Proteomics* **19**, 1058–1069 (2020).
28. Yuste-Checa, P., Bracher, A. & Hartl, F. U. The chaperone Clusterin in neurodegeneration—friend or foe?. *BioEssays* **44**, 2100287 (2022).
29. Feingold, K. R. Introduction to lipids and lipoproteins. In *Endotext* (eds Feingold, K. R. *et al.*) (MDText.com, Inc., 2000).
30. Crescitelli, R., Lässer, C. & Lötvall, J. Isolation and characterization of extracellular vesicle subpopulations from tissues. *Nat. Protoc.* **16**, 1548–1580 (2021).
31. Gomes, D. E. & Witwer, K. W. L1CAM-associated extracellular vesicles: A systematic review of nomenclature, sources, separation, and characterization. *J. Extracell. Bio* **1**, e35 (2022).
32. Norman, M. *et al.* L1CAM is not associated with extracellular vesicles in human cerebrospinal fluid or plasma. *Nat. Methods* **18**, 631–634 (2021).
33. Clos-Sansalvador, M., Monguió-Tortajada, M., Roura, S., Franquesa, M. & Borràs, F. E. Commonly used methods for extracellular vesicles' enrichment: Implications in downstream analyses and use. *Eur. J. Cell Biol.* **101**, 151227 (2022).
34. Li, M. *et al.* Isolation of exosome nanoparticles from human cerebrospinal fluid for proteomic analysis. *ACS Appl. Nano Mater.* **4**, 3351–3359 (2021).
35. Arab, T. *et al.* Characterization of extracellular vesicles and synthetic nanoparticles with four orthogonal single-particle analysis platforms. *J. Extracell. Vesicles* **10**, e12079 (2021).
36. Newman, L. A., Useckaite, Z. & Rowland, A. Addressing MISEV guidance using targeted LC-MS/MS: A method for the detection and quantification of extracellular vesicle-enriched and contaminant protein markers from blood. *J. Extracell. Bio* **1**, e56 (2022).
37. Hayashi, N. *et al.* Proteomic analysis of exosome-enriched fractions derived from cerebrospinal fluid of amyotrophic lateral sclerosis patients. *Neurosci. Res.* **160**, 43–49 (2020).
38. Krušić Alić, V. *et al.* Extracellular vesicles from human cerebrospinal fluid are effectively separated by sepharose CL-6B—Comparison of four gravity-flow size exclusion chromatography methods. *Biomedicines* **10**, 785 (2022).
39. Hirschberg, Y. *et al.* Characterising extracellular vesicles from individual low volume cerebrospinal fluid samples, isolated by SmartSEC. *J. Extracell. Bio* **1**, e55 (2022).
40. Bath, T. S. *et al.* Protein aggregation capture on microparticles enables multipurpose proteomics sample preparation. *Mol. Cell. Proteomics* **18**, 1027–1035 (2019).

Acknowledgements

This work was supported by the Academy of Finland under Grant number 332789; and Finnish Foundation of Veterinary Research with a scholarship. Mass spectrometry-based proteomic analyses were performed by the Proteomics Core Facility, Department of Immunology, University of Oslo/Oslo University Hospital, which is supported by the Core Facilities program of the South-Eastern Norway Regional Health Authority. This core facility is also a member of the National Network of Advanced Proteomics Infrastructure (NAPI), which is funded by the Research Council of Norway INFRASTRUKTUR-program (project number: 295910). Nanoparticle tracking analysis was performed at the University of Helsinki EV core, and TEM imaging at the Helsinki Electron Microscopy Core Unit. NanoFCM analysis was done at NanoFCM co., Ltd. We also thank Ninna Koho for helping us with the laboratory work.

Author contributions

Conceptualisation: P.K., J.K., T.S.J., T.A.N., T.W. and L.M. Methodology: P.K., J.K., T.S.J., T.A.N., C.B., and R.T. Data analysis and writing the original manuscript: P.K. and J.K. Writing (review and editing): P.K., J.K., T.S.J., T.A.N., C.B., R.T., T.W., and L.M. Visualisation: P.K. and J.K. Project administration and funding acquisition: T.S.J. All authors have read and agreed to the published version of the manuscript.

Competing interests

The authors declare no competing interests.

Additional information

Supplementary Information The online version contains supplementary material available at <https://doi.org/10.1038/s41598-023-36706-z>.

Correspondence and requests for materials should be addressed to P.K.

Reprints and permissions information is available at www.nature.com/reprints.

Publisher's note Springer Nature remains neutral with regard to jurisdictional claims in published maps and institutional affiliations.



Open Access This article is licensed under a Creative Commons Attribution 4.0 International License, which permits use, sharing, adaptation, distribution and reproduction in any medium or format, as long as you give appropriate credit to the original author(s) and the source, provide a link to the Creative Commons licence, and indicate if changes were made. The images or other third party material in this article are included in the article's Creative Commons licence, unless indicated otherwise in a credit line to the material. If material is not included in the article's Creative Commons licence and your intended use is not permitted by statutory regulation or exceeds the permitted use, you will need to obtain permission directly from the copyright holder. To view a copy of this licence, visit <http://creativecommons.org/licenses/by/4.0/>.

© The Author(s) 2023